


Superradiance-to-Polariton Crossover of Wannier Excitons with Multiple Resonances

Mitsuyoshi Takahata, Koichiro Tanaka, and Nobuko Naka*

Department of Physics, Kyoto University, Kitashirakawa-Oiwake-cho, Sakyo-ku, Kyoto 606-8502, Japan

 (Received 18 July 2018; published 24 October 2018)

We demonstrated the superradiance-to-polariton crossover of the blue excitons in Cu_2O by varying the sample thicknesses instead of controlling the cavity quality factor. The crossover behavior was compared with unprecedented calculations based on the nonlocal optical response theory with the inclusion of three exciton resonances. The crossover thickness, found to be 177 ± 2 nm, was smaller than the predicted value for a single resonance by a factor of 5. The fact that there was much larger longitudinal-transverse splitting (40 ± 5 meV) than in the bulk implies a surprisingly fast radiative recombination even without a cavity structure.

DOI: [10.1103/PhysRevLett.121.173604](https://doi.org/10.1103/PhysRevLett.121.173604)

Exploring many-body cooperative phenomena remains the central theme of quantum science with rapidly growing demands for ultrafast optical switches and high-precision atomic clocks [1]. A well-known example is the use of superradiance [2–5], where an ensemble of mutually phase-coherent atoms decay significantly faster than individual atoms. The system behaves as a single bosonic mode although it is a collection of two-level atoms. A wave function of excitons confined in microspheres and in a semiconductor slab is analogous to such a collective-state wave function of atoms. The maximum radiative decay rate is expected for a material size of approximately half a wavelength [6,7], as well as when the electromagnetic waveform and the wave function of the quantized exciton center-of-mass (c.m.) motion are phase matched. The exciton superradiance [8,9] can be further enhanced when embedded in a microcavity [10], but it is superseded by quasistationary exciton-polariton modes in a strong coupling regime [11,12]. Such a crossover has been already observed, e.g., for quantum dots [13] in a planar cavity by changing the quality factor, and later interpreted as a transition from the Purcell enhancement to vacuum Rabi splitting [14].

In 1995 [15], Björk *et al.* proposed that the crossover for confined excitons, regardless of the Frenkel or Wannier-Mott types, is expected also for a varying slab thickness without cavity [see Fig. 1(a)]. Increasing the thickness corresponds to an increase in the number of dipoles in phase that are localized or delocalized at the constituent atoms, toward the strong coupling regime. Upon increasing the size, the decay rate decreases beyond the crossover point, provided that the radiative rate of an exciton polariton is considered as the inverse of the propagation time through the slab [16]. The thick line in Fig. 1(a) represents the highest radiative mode for a given thickness, which shows the maximum radiative rate near the Rabi frequency ($\Delta_{\text{Rabi}}/\hbar$) [15], whereas the gray region indicates the

existence of subradiant modes [15,17]. In Fig. 1(b), the radiative energy, or the energy of the highest radiative mode is shown by the thick lines. It coincides (or crosses) with the bulk energy, $\hbar\omega_{\text{bulk}}$, below the crossover thickness, and otherwise splits into the upper and lower branch polaritons

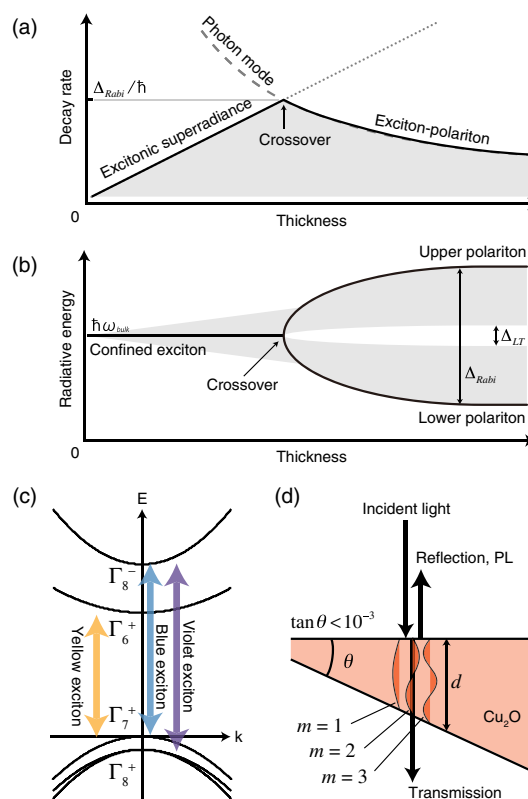


FIG. 1. Schematic of excitonic superradiance to exciton-polariton crossover in (a) decay rate and (b) resonance energy [15]. The solid lines trace the points of the maximum decay rates, and the gray region represents subradiant modes. (c) Band structure of Cu_2O . (d) Schematic of the Cu_2O film.

separated by Δ_{Rabi} . The subradiant modes (the gray regions) are separated by the longitudinal-transverse (LT) splitting energy, Δ_{LT} [15,17].

In this Letter, we report the first experimental observation of the crossover from excitonic superradiance to exciton-polariton under thickness control, by using Wannier-Mott excitons in Cu_2O [18]. Despite the advances in theory, achieving the crossover condition has been impossible for over two decades. The crossover thickness is approximately given by $d_{\text{cross}} = 4c\hbar/(n_b\Delta_{\text{Rabi}})$ [15], where c is the light speed in vacuum and n_b is the refractive index of the material. For a typical dipole-allowed transition, d_{cross} is on the order of several or tens of micrometers, far exceeding the coherence length of excitations in a material. This impedes the collective evolution of macroscopic dipoles spreading over d_{cross} .

In contrast to the weakly dipole-allowed “yellow” exciton series in Cu_2O with stringent interests [19–27], we focused on the blue and violet excitons [18,28] involving the second conduction band [see Fig. 1(c)]. The Rabi splitting energy (280 meV [28]) for the bulk blue exciton is 70 times larger than in GaAs [29] and 3 times larger than in CuCl [30]. This exceptionally strong radiative coupling reduces the crossover thickness down to an observable range of $< 1 \mu\text{m}$. Our thin film was, in fact, grown between wedge-shaped substrates [see Fig. 1(d)], and the radiative coupling was further enhanced by multiple reflections at the interfaces [17]. Because of further enhancements by multiple resonances derived from higher lying states including the excited ($2s$) blue exciton and the violet exciton, the crossover was expected at a thickness below 200 nm. In what follows, we perform a detailed examination of the absorption and photoluminescence (PL) spectra of the blue exciton, and compare them with theory, including new extensions to multiple resonances.

We used Cu_2O thin films grown between sapphire substrates by the melt method [31]. The sample was mounted in a static-gas type cryostat (Oxford, OptistatSXM) and irradiated by visible light from a supercontinuum source (Fianium, WhiteLase micro). In our custom-built confocal optical system [32], we selected the position ($2 \times 2 \mu\text{m}^2$) of the desired film thickness under an aspherical objective lens (Thorlabs, C671TME-A) by a triaxial piezoelectric actuator (Attocube, ANPx51, ANPz51). The detection was made by a charge-coupled-device camera at the exit port of a monochromator (Nikon, CT-25T JASCO). Absorption spectra were obtained by subtracting the measured reflection and transmission spectra from unity. The photoluminescence was measured using the same detection setup under weak continuous-wave excitations at a photon energy of 3.05 eV (Thorlabs, LD5146-101S), which is well above the resonance energies of the blue exciton ($\hbar\omega_{1sb} = 2.576 \text{ eV}$) and the violet exciton ($\hbar\omega_{1sv} = 2.703 \text{ eV}$) [28].

Figures 2(a) and 2(b) show the absorption spectra in the region of the blue and violet excitons, for film thicknesses

ranging from 22 to 154 nm and from 170 to 400 nm, respectively. Around the bulk energies of the blue and violet excitons, as indicated by the dashed lines, several peaks are observed. The peak positions around $\hbar\omega_{1sb}$ are marked by diamonds, and plotted as a function of thickness d in Fig. 2(c). The energy positions of the absorption peaks exhibited qualitatively different thickness dependence in the thin and thick regions, indicating different types of light-matter interactions. Starting from the thin region, the initially single peak (marked by the dashed-line circle) splits with a maximum separation of 60 meV at a thickness of 70 nm, and then merges and crosses $\hbar\omega_{1sb}$ (the full-line circle) at 80 nm. The energy shift is derived from the spatial phase matching between the c.m. wave function of the confined excitons and the spatial mode of the resonant light wave. In the thicker region ($d > 100 \text{ nm}$), the peaks are split into two or more, and no crossing of the peaks across $\hbar\omega_{1sb}$ is observed. The two major energy positions correspond to the upper and lower branch polaritons, separated by $\Delta_{1sb}^{\text{LT}} = \Delta_{\text{Rabi}}^2/(4\hbar\omega_{1sb})$ [33]. Roughly speaking, the boundary at $d \sim 80\text{--}200 \text{ nm}$ between the different

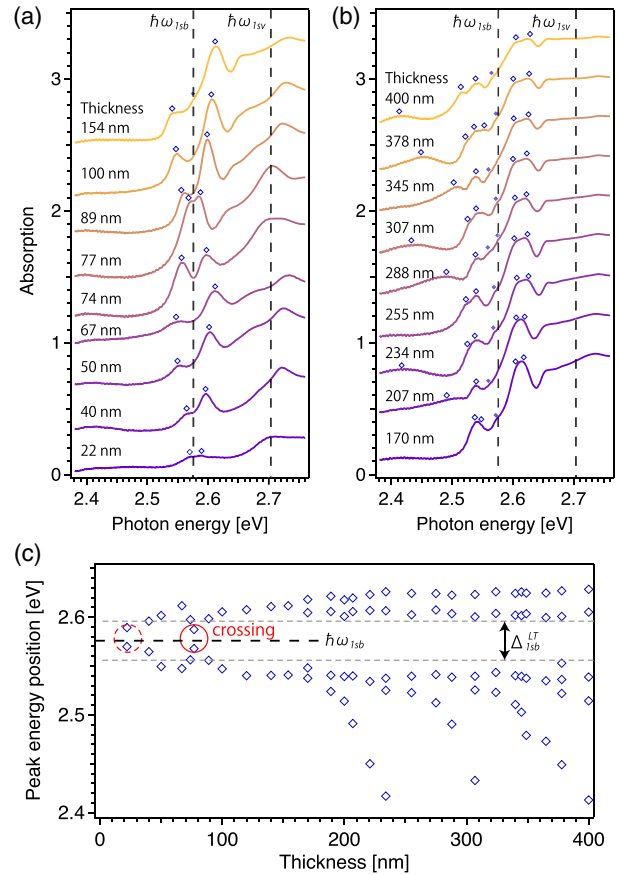


FIG. 2. (a),(b) Absorption spectra of a Cu_2O thin film at 9 K at different thicknesses. Dashed lines indicate resonance energies of the blue ($\hbar\omega_{1sb}$) and violet ($\hbar\omega_{1sv}$) excitons in a bulk crystal. (c) Peak energies of the absorption as a function of film thickness.

behaviors indicates a crossover point from excitonic super-radiance to exciton polariton.

We will first discuss the detailed energy positions observed in the absorption spectra. The shifts from the bulk energies originate from the nonlocality between the polarization and the electric field of the light beyond the long-wavelength approximation [7,34,35]. A case with a thickness region much smaller than the crossover point was reported in our recent publication for the yellow exciton in Cu₂O [32]. We used the nonlocal optical response theory [7,34,36], accounting for the excitonic superradiance [8,9]. Thus, we calculated the exciton resonance energy using the susceptibility described as

$$\chi(z, z', \omega) = \sum_j \frac{2\Delta_j^{\text{LT}}}{d} \times \sum_m \frac{\sin(\frac{m\pi}{d}z) \sin(\frac{m\pi}{d}z')}{\hbar\omega_j + \frac{\hbar^2}{2M}(\frac{m\pi}{d})^2 - \hbar\omega - i\hbar\gamma_{nr}/2}, \quad (1)$$

where z is the distance along the film depth, $M = 3.0m_0$ is the effective mass of the excitons (assumed to be equal to that of the 1s yellow exciton for simplicity [37]), m is the number of antinodes of the c.m. wave function [see Fig. 1(d)], and $\gamma_{nr} = 20$ meV is the nonradiative decay rate [38]. It is seen that exciton polaritons interact with photons locally, by simply observing that the right-hand side of the equation reduces to $\delta(z - z')$ in the limit of $d \rightarrow \infty$. The contribution of the 1s and 2s blue excitons and the 1s violet exciton is included in the sum over j [36,39]. This opposes previous publications that deal only with a single exciton level in the discussions of crossover [17,32].

The lines in Fig. 3(a) are the calculated energy positions, with the colors representing the radiative coupling strength. The coupling strength is given by the radiative width obtained as the imaginary part of the resonance energy [32]. The LT splitting energies were chosen as $\Delta_{1sb}^{\text{LT}} = 40$, $\Delta_{2sb}^{\text{LT}} = \Delta_{1sb}^{\text{LT}}(f_{2sb}/f_{1sb}) = 5$, and $\Delta_{1sv}^{\text{LT}} = \Delta_{1sb}^{\text{LT}}(f_{1sv}/f_{1sb}) = 70$ meV, where $f_{1sb} = 1.2 \times 10^{-2}$ [28], $f_{2sb} = f_{1sb}/8$ [21], and $f_{1sv} = 2.1 \times 10^{-2}$ [28] are the oscillator strengths of the blue and violet excitons. We found that the value of the LT splitting energy affects the separation between the subradiant modes and energy positions of the lower branch polaritons. We obtained $\Delta_{1sb}^{\text{LT}} = 40 \pm 5$ meV to best reproduce the experimental points.

As shown in the inset of Fig. 3(a), the radiative width of the lowest ($m = 1$) mode is most enhanced at the thickness of 30 nm. The energy shift of the second mode ($m = 2$) results in the crossing across the bulk energy at the thickness of 80 nm as indicated by the full-line circle. No crossing was found for the $m \geq 3$ modes, where the calculated radiative width reached the highest value of 0.6 eV for $m = 3$ at around 177 nm [the dotted circle in Fig. 3(a)]. Comparing this with Fig. 1(a) and considering

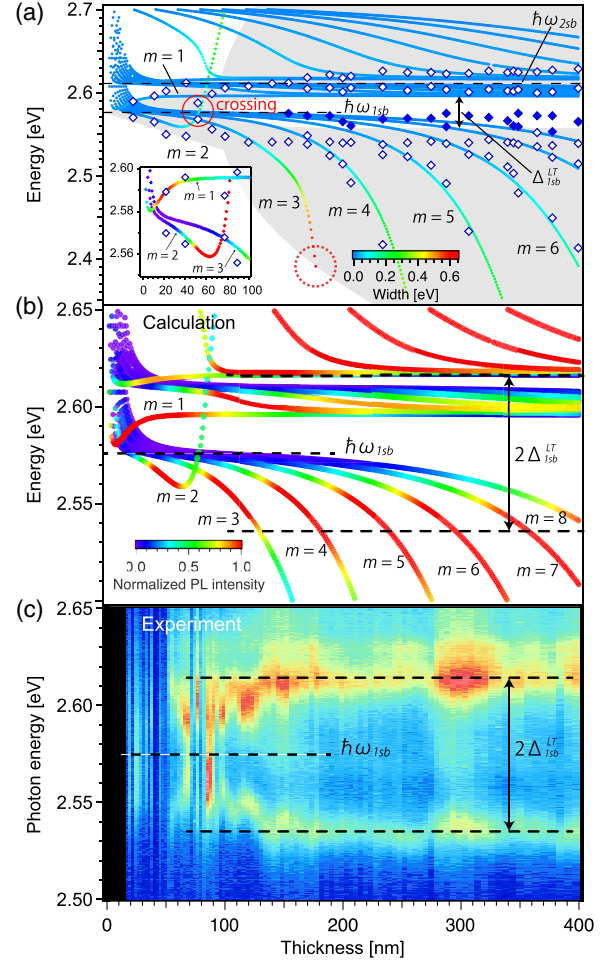


FIG. 3. (a) Calculated resonance energies (lines) in comparison with the experimental data (diamonds). The color of the lines indicates the radiative width. The inset highlights the $m = 1, 2, 3$ modes with rescaled colors. (b) Resonance energies with the calculated PL intensities represented by the color. (c) Contour plot of the measured PL spectra at 4.5 K.

the error in Δ_{1sb}^{LT} suggests that the crossover thickness is $d_{\text{cross}} = 177 \pm 2$ nm. The corresponding radiative lifetime is 1.1 fs, which is, in fact, shorter than the inverse of the Rabi frequency, 1.6 fs, and implies a strongly enhanced light-matter coupling. We should note that the high radiative enhancement is due to the inclusion of the violet exciton.

Unfortunately, the highest radiative mode does not appear as a peak in the absorption spectra because of extensive broadening. Nevertheless, the following facts are observed leading to $d_{\text{cross}} = 160 \pm 20$ nm experimentally: (i) the $m = 3$ mode lowers its energy up to $d = 140$ nm beyond the crossing of the $m = 2$ mode, which indicates super-radiance, and (ii) the $m = 4$ mode clearly shows splitting into the subradiant polariton branch above $d = 180$ nm.

If we associate the calculated blue lines with the data points (open diamonds), a good agreement is found in

terms of the large separation between the upper and lower branches and the small splitting in the upper branch, which is ascribed to the $2s$ blue exciton at $\hbar\omega_{2sb} = 2.610$ eV. It can be seen that the positions of the small shoulder near $\hbar\omega_{1sb}$ are subradiant modes as indicated by solid diamonds. The separation of the gap above these subradiant modes agrees with the LT splitting, $\Delta_{1sb}^{LT} = 40$ meV. The fact that this value far exceeds the bulk value (7.6 meV) is presumably because of the long coherence length along the film depth. This enhancement strengthens the light-matter coupling and thus helps to reduce the crossover thickness down to less than 200 nm.

Next, we considered the case of the PL process to confirm some modes with higher radiative rates. The calculated radiative rate γ_r for the blue exciton varies below and above the nonradiative rate. Therefore, the strongest PL peak intensities do not necessarily come from the highest radiative mode. We recently discovered the PL of bulk blue excitons and that the spectrum could be reproduced by a Lorentzian [38]: $I(\hbar\omega, d, m) = G\gamma_r(d, m) / [\{\hbar\omega(d, m) - \hbar\omega_0\}^2 + \{\hbar\gamma_r(d, m)/2 + \hbar\gamma_{nr}/2\}^2]$. The exciton generation yield G is independent of d because the penetration length (40 nm) [18] is smaller than the thickness. Mathematically, the peak intensity $I(\hbar\omega_0)$ shows its maximum value when $\gamma_r = \gamma_{nr}$. Physically, for a radiative rate much higher than the nonradiative rate, the PL peak broadens and reduces its height. Consequently, the maximum peak intensity of PL appears for modes with a moderate coupling strength rather than those of the strongest coupling strength.

The colors of the lines in Fig. 3(b) represent the calculated PL peak intensity, $I(\hbar\omega_0)$, normalized at each thickness. High PL peak intensities are expected for the $m = 1$ mode for $d < 100$ nm and along the two horizontal lines separated by $2\Delta_{1sb}^{LT}$ for $d > 100$ nm. This splitting is slightly larger than that expected for absorption, as it is highlighted for the condition $\gamma_r = \gamma_{nr}$. In particular, the PL peak intensity is expected to be comparable for the upper and lower branches despite the fact that their separation is

larger than the thermal energy and the accumulation of the exciton population is expected at the lower branch.

Figure 3(c) shows a contour plot of thickness dependence of the measured PL spectra. As predicted, the separation of the upper and lower branches agreed with $2\Delta_{1sb}^{LT}$ and was larger than that for absorption. The PL peak intensity was stronger at the upper branch than at the lower branch. This reversal in the PL peak intensity means that the upper branch modes have comparable radiative coupling strength as the lower ones, and that the PL is further enhanced by the degeneracy of several of the upper branch modes. The overall agreement between Figs. 3(a)–3(c) is excellent, and this fact strengthens our attribution of the crossover thickness to 177 ± 2 nm.

Finally, we calculated the spatial distributions of the electric field and the polarization along the film depth in order to understand the relationship between crossover and the nonlocality. The calculated results as a function of the depth for film thicknesses of (a) 10, (b) 50, (c) 100, and (d) 200 nm are shown in Figs. 4(a)–4(d). Because the mode of the highest coupling varies depending on the thickness, we chose such a mode for each thickness. For thicknesses smaller than 50 nm, the distribution of the electric field is very different from that of the polarization [Figs. 4(a) and 4(b)], particularly near the sample edges. As the thickness increases, these two distributions become closer [Fig. 4(c)] until they are almost the same [Fig. 4(d)]. This result means that similarity (dissimilarity) between spatial distributions of the electric field and polarization leads to qualitatively different response for a thickness below (above) the crossover point, respectively.

According to our calculations, the spatial structure of the internal electric field in the thin region [Fig. 4(a)] is close to a free photon in a sense that the amplitude does not depend on the position. On the other hand, the spatial structure in the thick region is closer to a cavity photon than a free photon, in the sense that the amplitude of the electric field has one or more nodes. This may be reasonable considering that the spatial distribution of the photon approaches that of

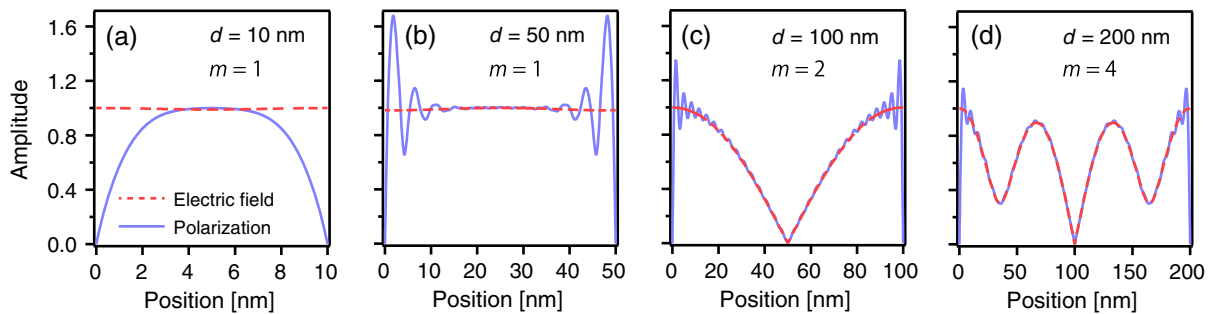


FIG. 4. (a)–(d) Spatial distributions of the electric field amplitude (dashed lines) and polarization amplitude (solid lines) for the maximum coupling mode at each thickness. The directions of the electric field and polarization are reversed at the middle point of the horizontal axis in (c) and (d).

the c.m. wave function of the confined excitons due to the strong light-matter interaction, although the cavity quality factor of the present sample is very low (~ 1).

To summarize, we have presented a clear observation of the superradiance-to-polariton crossover in the absorption and PL spectra of the blue exciton in Cu_2O . The extracted parameters (crossover thickness at 177 ± 2 nm and LT splitting energy of 40 ± 5 meV) indicated a faster radiative decay compared to that expected for a single resonance. Near the crossover thickness, we showed that the electric field distribution of photons is similar to the cavity photon, indicating a new type of confined photons. This suggests that cavity polaritons were formed without a cavity structure, due to the strong coupling to the exciton c.m. wave functions. We believe that our scheme can provide a novel way of manipulating strong light-matter interactions, and can have vast applications in areas such as Bose-Einstein condensates [40–42], superfluid [12], polariton lasing [43], and quantum information processing [44], by using the polariton superradiant states.

We thank Satoshi Hashimoto (Osaka Prefecture University) for the Cu_2O film growth through collaboration with Teruya Ishihara (Tohoku University) and Hiroshi Ajiki (Tokyo Denki University) for helpful comments on non-locality. This work was partially supported by a Grant-in-Aid for Scientific Research (C) (Grant No. 26400317) and a Grant-in-Aid for Scientific Research (B) (Grant No. 17H02910) from JSPS, Japan.

*naka@scphys.kyoto-u.ac.jp

- [1] M. A. Norcia, J. R. K. Cline, J. A. Muniz, J. M. Robinson, R. B. Hutson, A. Goban, G. E. Marti, J. Ye, and J. K. Thompson, Frequency Measurements of Superradiance from the Strontium Clock Transition, *Phys. Rev. X* **8**, 021036 (2018).
- [2] R. H. Dicke, Coherence in spontaneous radiation processes, *Phys. Rev.* **93**, 99 (1954).
- [3] N. Skribanowitz, I. P. Herman, J. C. MacGillivray, and M. S. Feld, Observation of Dicke Superradiance in Optically Pumped HF Gas, *Phys. Rev. Lett.* **30**, 309 (1973).
- [4] C. Bradac, M. T. Johnsson, M. van Breugel, B. Q. Baragiola, R. Martin, M. L. Juan, G. K. Brennen, and T. Volz, Room-temperature spontaneous superradiance from single diamond nanocrystals, *Nat. Commun.* **8**, 1205 (2017).
- [5] A. I. Chumakov, A. Q. R. Baron, I. Sergueev, C. Strohm, O. Leupold, Y. Shvyda'ko, G. V. Smirnov, R. Ruffer, Y. Inubushi, M. Yabashi, K. Tono, T. Kudo, and T. Ishikawa, Superradiance of an ensemble of nuclei excited by a free electron laser, *Nat. Phys.* **14**, 261 (2018).
- [6] G. Björk, S. Pau, J. Jacobson, and Y. Yamamoto, Wannier exciton superradiance in a quantum-well microcavity, *Phys. Rev. B* **50**, 17336 (1994).
- [7] K. Cho, *Optical Response of Nanostructures: Microscopic Nonlocal Theory* (Springer, New York, 2003).
- [8] T. Itoh, M. Furumiya, and T. Ikehara, Size-dependent radiative decay time of confined excitons in CuCl microcrystals, *Solid State Commun.* **73**, 271 (1990).
- [9] K. Misawa, H. Yao, T. Hayashi, and T. Kobayashi, Size effects on luminescence dynamics of CdS microcrystallites embedded in polymer films, *Chem. Phys. Lett.* **183**, 113 (1991).
- [10] J. M. Gérard, B. Sermage, B. Gayral, B. Legrand, E. Costard, and V. Thierry-Mieg, Enhanced Spontaneous Emission by Quantum Boxes in a Monolithic Optical Microcavity, *Phys. Rev. Lett.* **81**, 1110 (1998).
- [11] J. Kasprzak, M. Richard, S. Kundermann, A. Baas, P. Jeambrun, J. M. J. Keeling, F. M. Marchetti, M. H. Szymańska, R. André, J. L. Staehli, V. Savona, P. B. Littlewood, B. Deveaud, and L. S. Dang, Bose-Einstein condensation of exciton polaritons, *Nature (London)* **443**, 409 (2006).
- [12] G. Lerario, A. Fieramosca, F. Barachati, D. Ballarini, K. S. Daskalakis, L. Dominici, M. D. Giorgi, S. A. Maier, G. Gigli, S. Kéna-Cohen, and D. Sanvitto, Room-temperature superfluidity in a polariton condensate, *Nat. Phys.* **13**, 837 (2017).
- [13] H. M. Gibbs, in *Optics of Semiconductors and Their Nanostructures*, edited by H. Kalt and M. Hetterich (Springer, Berlin, 2004), p. 189.
- [14] G. Khitrova, H. M. Gibbs, M. Kira, S. W. Koch, and A. Scherer, Vacuum Rabi splitting in semiconductors, *Nat. Phys.* **2**, 81 (2006).
- [15] G. Björk, S. Pau, J. M. Jacobson, H. Cao, and Y. Yamamoto, Excitonic superradiance to exciton-polariton crossover and the pole approximations, *Phys. Rev. B* **52**, 17310 (1995).
- [16] W. J. Rappel, L. F. Feiner, and M. F. H. Schuurmans, Exciton-polariton picture of the free-exciton lifetime in GaAs , *Phys. Rev. B* **38**, 7874 (1988).
- [17] M. Bamba and H. Ishihara, Crossover of exciton-photon coupled modes in a finite system, *Phys. Rev. B* **80**, 125319 (2009).
- [18] B. K. Meyer, A. Polity, D. Reppin, M. Becker, P. Hering, P. J. Klar, T. Sander, C. Reindl, J. Benz, M. Eickhoff, C. Heiliger, M. Heinemann, J. Blasing, A. Krost, S. Shokovets, C. Müller, and C. Ronning, Binary copper oxide semiconductors: From materials towards devices, *Phys. Status Solidi B* **249**, 1487 (2012).
- [19] E. F. Gross and N. A. Karryev, Opticheskii spektr eksitonov, *Dokl. Akad. Nauk SSSR* **84**, 471 (1952).
- [20] K. Yoshioka, E. Chae, and M. Kuwata-Gonokami, Transition to a Bose-Einstein condensate and relaxation explosion of excitons at sub-Kelvin temperatures, *Nat. Commun.* **2**, 328 (2011).
- [21] T. Kazimierczuk, D. Fröhlich, S. Scheel, H. Stolz, and M. Bayer, Giant Rydberg excitons in the copper oxide Cu_2O , *Nature (London)* **514**, 343 (2014).
- [22] K. Iwamitsu, S. Aihara, M. Okada, and I. Akai, Bayesian analysis of an excitonic absorption spectrum in a Cu_2O thin film sandwiched by paired MgO plates, *J. Phys. Soc. Jpn.* **85**, 094716 (2016).
- [23] F. Schweiner, J. Ertl, J. Main, and G. Wunner, and C. Uihlein, Exciton-polaritons in cuprous oxide: Theory and comparison with experiment, *Phys. Rev. B* **96**, 245202 (2017).

- [24] S. Zielińska-Raczyńska, D. Ziemkiewicz, and G. Czajkowski, Magneto-optical properties of Rydberg excitons: Center-of-mass quantization approach, *Phys. Rev. B* **95**, 075204 (2017).
- [25] H. Stolz, F. Schöne, and D. Semkat, Interaction of Rydberg excitons in cuprous oxide with phonons and photons: optical linewidth and polariton effect, *New J. Phys.* **20**, 023019 (2018).
- [26] S. O. Krüger and S. Scheel, Waveguides for Rydberg excitons in Cu_2O from strain traps, *Phys. Rev. B* **97**, 205208 (2018).
- [27] J. Mund, D. Fröhlich, D. R. Yakovlev, and M. Bayer, High-resolution second harmonic generation spectroscopy with femtosecond laser pulses on excitons in Cu_2O , *Phys. Rev. B* **98**, 085203 (2018).
- [28] J. Schmutzler, D. Fröhlich, and M. Bayer, Signatures of coherent propagation of blue polaritons in Cu_2O , *Phys. Rev. B* **87**, 245202 (2013).
- [29] C. Weisbuch, M. Nishioka, A. Ishikawa, and Y. Arakawa, Observation of the Coupled Exciton-Photon Mode Splitting in a Semiconductor Quantum Microcavity, *Phys. Rev. Lett.* **69**, 3314 (1992).
- [30] G. Oohata, T. Nishioka, D. Kim, H. Ishihara, and M. Nakayama, Giant Rabi splitting in a bulk CuCl microcavity, *Phys. Rev. B* **78**, 233304 (2008).
- [31] N. Naka, S. Hashimoto, and T. Ishihara, Thin films of single-crystal cuprous oxide grown from the melt, *Jpn. J. Appl. Phys.* **44**, 5096 (2005).
- [32] M. Takahata, K. Tanaka, and N. Naka, Nonlocal optical response of weakly confined excitons in Cu_2O mesoscopic films, *Phys. Rev. B* **97**, 205305 (2018).
- [33] A. Kavokin and B. Gil, GaN microcavities: Giant Rabi splitting and optical anisotropy, *Appl. Phys. Lett.* **72**, 2880 (1998).
- [34] H. Ishihara, J. Kishimoto, and K. Sugihara, Anomalous mode structure of a radiation-exciton coupled system beyond the long-wavelength approximation regime, *J. Lumin.* **108**, 343 (2004).
- [35] M. Ichimiya, M. Ashida, H. Yasuda, H. Ishihara, and T. Itoh, Observation of Superradiance by Nonlocal Wave Coupling of Light and Excitons in CuCl Thin Films, *Phys. Rev. Lett.* **103**, 257401 (2009).
- [36] T. Kinoshita and H. Ishihara, Radiative coupling of A and B excitons in ZnO , *Phys. Rev. B* **94**, 045441 (2016).
- [37] G. Dasbach, D. Fröhlich, R. Klieber, D. Suter, M. Bayer, and H. Stolz, Wave-vector-dependent exchange interaction and its relevance for the effective exciton mass in Cu_2O , *Phys. Rev. B* **70**, 045206 (2004).
- [38] M. Takahata and N. Naka (to be published).
- [39] The yellow exciton (below 2.172 eV) and the green exciton (below 2.304 eV) are far enough apart and their oscillator strengths are negligibly small.
- [40] L. W. Clark, A. Gaj, L. Feng, and C. Chin, Collective emission of matter-wave jets from driven Bose-Einstein condensates, *Nature (London)* **551**, 356 (2018).
- [41] A. U. J. Lode, F. S. Diorico, R. G. Wu, P. Mognini, L. Papariello, R. Lin, C. Lvque, L. Exl, M. C. Tsatsos, R. Chitra, and N. J. Mauser, Many-body physics in two-component Bose-Einstein condensates in a cavity: fragmented superradiance and polarization, *New J. Phys.* **20**, 055006 (2018).
- [42] L. Chen, P. Wang, Z. Meng, L. Huang, H. Cai, D.-W. Wang, S.-Y. Zhu, and J. Zhang, Experimental Observation of One-Dimensional Superradiance Lattices in Ultracold Atoms, *Phys. Rev. Lett.* **120**, 193601 (2018).
- [43] S. Kena-Cohen and S. R. Forrest, Room-temperature polariton lasing in an organic single-crystal microcavity, *Nat. Photonics* **4**, 371 (2010).
- [44] D. D. Solnyshkov, O. Bleu, and G. Malpuech, All optical controlled-NOT gate based on an exciton-polariton circuit, *Superlattices Microstruct.* **83**, 466 (2015).